Pyrrolo[2,3-*d*]pyrimidine Thymidylate Synthase Inhibitors: Design and Synthesis of One-Carbon Bridge Derivatives

Kazuyoshi Aso,*[,a] Yumi Imai,[a] Koichi Yukishige,[b] Koichiro Ootsu,[c] and Hiroshi Akimoto[d]

Medicinal Chemistry Research Laboratories,[a] Takeda RABICS[c] and Intellectual Property Department,[d] Takeda Chemical Industries, Ltd., 2–17–85 Jusohonmachi, Yodogawa-ku, Osaka 532–8686, Japan and Pharmaceutical Business Development Department,[b] Takeda Chemical Industries, Ltd., 4–1–1 Doshomachi, Chuo-ku, Osaka 540–8645, Japan.
Received April 18, 2001; accepted July 23, 2001

A series of novel pyrrolo[2,3-*d*]pyrimidine derivatives was designed and synthesized as thymidylate synthase (TS) inhibitors. Molecular design was performed on the human TS complex model built on the basis of the reported structure of TS-deoxyuridinemonophosphate (dUMP)-CB3717 ternary complex. From a docking study, we expected that a one-carbon bridge between pyrrolo[2,3-*d*]pyrimidine and an aromatic ring was suitable. Moreover, we found that the bridge carbon could be replaced with an alkyl group to fill out the unoccupied space. Based on this design, we synthesized five pyrrolo[2,3-*d*]pyrimidine derivatives with one-carbon bridge and evaluated their TS inhibitory activities. All synthesized compounds inhibited TS more potently than compound 2 (LY231514), and the C8-ethyl analogue (7) showed a remarkable inhibitory activity against TS (IC_{50}=0.017 μM).

Key words pyrrolo[2,3-*d*]pyrimidine; thymidylate synthase (TS); molecular design; ternary complex

Thymidylate synthase (TS) catalyzes the conversion of 2′-deoxyuridine-5′-monophosphate (dUMP) to 2′-deoxythymidine-5′-monophosphate (dTMP) and is essential for *de novo* DNA biosynthesis.[1)] Thus, TS has long been recognized as an important target for cancer chemotherapy, and several TS inhibitors have emerged as clinical candidates.[2)]

We previously reported that *N*-[4-[3-(2,4-diamino-7*H*-pyrrolo[2,3-*d*]pyrimidin-5-yl)propyl]benzoyl]-L-glutamic acid (**1**, TNP-351) exhibited potent antitumor activities against various solid tumors and methotrexate (MTX) resistant mouse lymphocytic leukemia *in vitro* and *in vivo*.[3—7)] After extensive chemical modification of pyrrolo[2,3-*d*]-pyrimidine antifolates,[8—12)] the 4-oxo compounds (**2**, **3**) were found to moderately inhibit TS (IC_{50}=4.7, 1.4 μM, respectively).[8)] Taylor and co-workers independently reported the synthesis and TS inhibitory activity of compound **2** (LY231514) as a 5,10-dideaza-5,6,7,8-tetrahydrofolic acid (DDATHF)[13)] analogue.[14)] Clinical trials of LY231514 are underway.[15)]

The 3D (three-dimensional) structure of *E. coli* TS–dUMP–CB3717 ternary complex has been determined by X-ray crystallography.[16)] The structural information of TS enabled us to design potent TS inhibitors of pyrrolo[2,3-*d*]pyrimidine using molecular modeling techniques. Agouron's group reported the drug design and synthesis of a new class of TS inhibitors by an iterative crystallographic analysis of an *E. coli* TS–dUMP–inhibitor ternary complex.[17)] Although their iterative process is a useful strategy for ligand design, it usually takes considerable time to isolate and to solve the crystallized structure of the complex. In addition, their design was carried out on TS from *E. coli*. The sequence of *E. coli* TS at the active site has high homology (75% identity) to the human sequence (Fig. 2), but we thought it would be advantageous for an accurate design to use a human TS model. Thus, to explore novel TS inhibitors we built a human TS–dUMP–inhibitor complex model on the basis of the reported *E. coli* TS–dUMP–CB3717 ternary complex.[16)] Here we report our design and the synthesis of unique pyrrolo[2,3-*d*]pyrimidine derivatives with one-carbon bridge and their potent inhibitory activities against TS.

Design When we started our research, the 3D structure of human TS was not available. Thus, the 3D model of human TS was built by comparative modeling techniques using the amino acid sequence of human TS and the crystal structure of the reported *E. coli* TS–dUMP–CB3717 ternary complex.[16,18)] After dUMP and CB3717 were docked manually according to the crystal structure, the energy of the complex model was minimized with moderate constraints on the backbone and dUMP.[19)] In human TS, the enzyme-ligand interactions might be altered by three replacements around the active site region [Glu82 (*E. coli*)→Ala (human), Trp83 (*E. coli*)→Asn (human) and Val262 (*E. coli*)→Met (human)]. (The numbering of the human TS model corresponds to that of *E. coli* TS.) The replacement of Trp83→Asn would introduce hydrogen-bonding sites, while the replacements of Glu82→Ala and Val262→Met would alter hydrophobic interactions. After our research was completed, three crystal structures of human TS complexed with its inhibitors have become accessible from the Protein Data Bank.[20)] Comparison of the crystal structures by superimposing the backbones demonstrated that the active site structure of our human TS model was consistent with that of the crystal structures and suitable for structure-based drug design.[21)]

We started the drug design by studying the binding mode of CB3717 in the human TS model (Fig. 3a). Its binding factors were speculated to include three hydrogen-bonding interactions between 2-NH_2 and Ala263, 3-NH and Asp169, and 4-O and Gly173. The *p*-aminobenzoyl and propargyl moieties contributed to the hydrophobic interactions with Ile79, Leu172, Pro175 and Phe176. Aromatic ring stacking interactions were also present between the quinazolinone and the pyrimidine of dUMP. In addition, a hydrophobic cavity surrounded by Glu58, Trp80 and the propargyl moiety was observed (Fig. 3b).

We then focused our attention on the design of novel pyrrolo[2,3-*d*]pyrimidine derivatives as TS inhibitors, based on the information from the human TS–dUMP–CB3717 ternary complex model. A docking study of compound **2** (LY231514) with the human TS model suggested that the hydrogen-bond between 4-O and Gly173 was absent while the

* To whom correspondence should be addressed. e-mail: Aso_Kazuyoshi@takeda.co.jp

hydrophobic interactions of the benzoyl moiety were preserved. These results led us to speculate that the pyrrolo[2,3-*d*]pyrimidine ring moved from the position of the quinazoline of CB3717, because the benzoyl moiety was accommodated into the hydrophobic pocket (Fig. 4). This could be caused by the replacement of the quinazoline ring with the pyrrolo[2,3-*d*]pyrimidine ring and the deletion of the propargyl moiety. Using this information, we replaced the two-carbon bridge of compound **2** with a one-carbon bridge (compound **4**) to restore the important binding factors, that is, three hydrogen-bonds (between 2-NH_2 and Ala263, 3-NH and Asp169, and 4-O and Gly173) and the hydrophobic interactions of the benzoyl moiety with the enzyme. Actually, when the binding mode of **4** in the human TS model was examined, three hydrogen-bonds of the pyrrolo[2,3-*d*]pyrimidine system, hydrophobic interactions of the benzene moiety, and ring stacking between the pyrimidine of dUMP and pyrrolo[2,3-*d*]pyrimidine, were observed similar to those for CB3717 (Fig. 6). The substitution of the thiophene ring for a benzene ring (**5**) led to similar interactions, but the hydrogen-bond length (3.46 Å) between 4-O and Gly173 was a little longer than that of **4** (3.04 Å). The hydrophobic interactions of the bridge chain moiety of compound **5** seemed enhanced, because the length between C8 and Glu58 was shortened (Fig. 6). Based on these considerations compounds **4** and **5** were expected to exhibit potent inhibitory activities against TS.

We further examined the ternary complex model of compound **4**, and found that there could be a hydrophobic space surrounded by Glu58, Trp80 and the bridge chain (Fig. 7). This space existed in the complex model of CB3717 and was not occupied by the propargyl moiety. Filling the space by a hydrophobic moiety was expected to stabilize the binding energy, thus we introduced a hydrophobic substituent at the 8-position of compound **4** [**6** (R=methyl), **7** (R=ethyl), **8** (R=vinyl)]. Each of the enantiomers of **6**—**8** were incorporated in the human TS complex model and examined. These models demonstrated that the length between each substituent at C8 and Glu58 (or Trp80) was shortened and the substituent filled the hydrophobic space efficiently, regardless of the absolute configuration of C8 (Figs. 7, 8). In addition, three hydrogen-bonds between the pyrrolo[2,3-*d*]pyrimidine system and TS were well preserved for **6**—**8** and the lengths of the hydrogen-bonds were equivalent to those of **4** (Fig. 8). These results suggested that both the enantiomers of compounds **6**—**8** could inhibit TS more potently than compound **4**.

Recently, a pyrrolo[2,3-*d*]pyrimidine antifolate with a sulfur bridge and potent inhibitory effect on TS were reported.[22] When this compound was docked into the human TS model, similar interactions were observed such as three hydrogen bonds and the ring stacking with dUMP. However, the sulfur bridge would not be important except for the role as a spacer. Our independently designed compounds are characterized by one carbon bridge, and the fact that they can adopt a hydrophobic substituent on the bridge carbon.

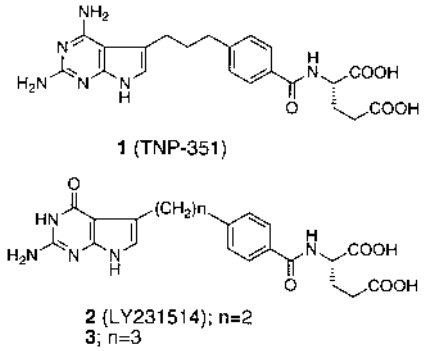

Fig. 1. Pyrrolo[2,3-*d*]pyrimidine Antifolates

Chemistry

The syntheses of compounds **4**—**8** are summarized in Charts 1 and 2. The key reaction was the synthesis of the pyrrolo[2,3-*d*]pyrimidine nucleus by the coupling of 2,6-diamino-4-hydroxypyrimidine with an acyclic precursor α-bromoaldehyde. This reaction was performed using the conditions reported by Secrist III,[23] with some modifications.

The key intermediates **10a** and **10b** for the syntheses of

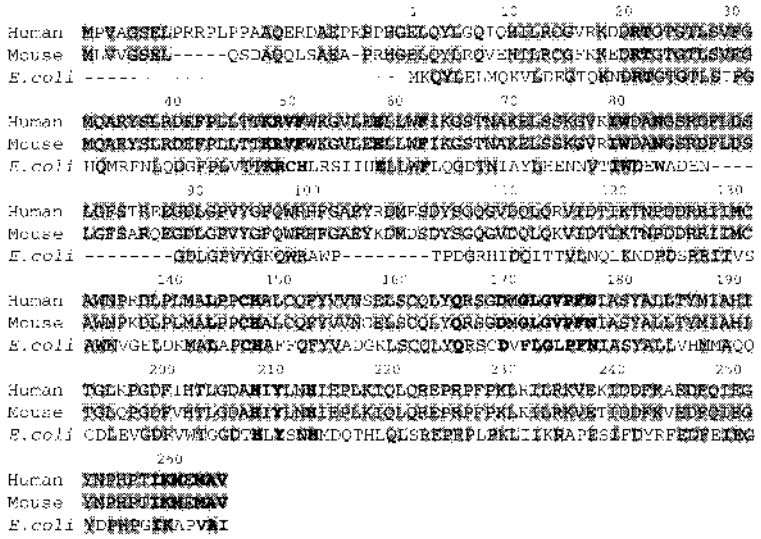

Fig. 2. Sequence Alignments of Human, Mouse and *E. coli* TS

The conserved residues are indicated by shaded boxes. The active site is defined as the region within a radius of 5 Å from the ligand in the crystal structure of *E. coli* TS ternary complex, and indicated with bold characters. The numbering corresponds to *E. coli* TS.

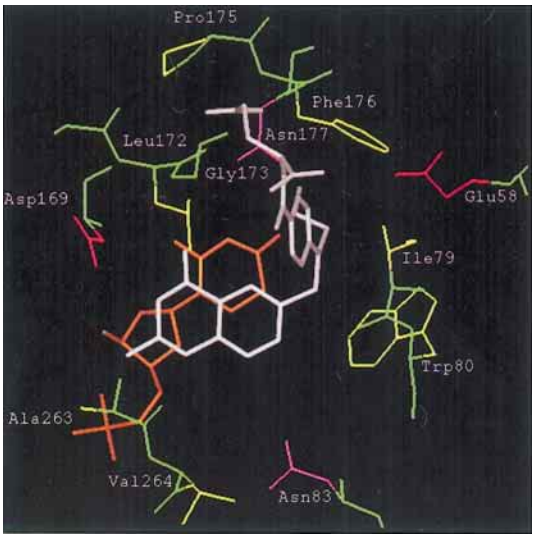

Fig. 3a. A Schematic Model for the Binding Mode of CB3717 with Human TS

CB3717 is shown by white wire model and dUMP by brown.

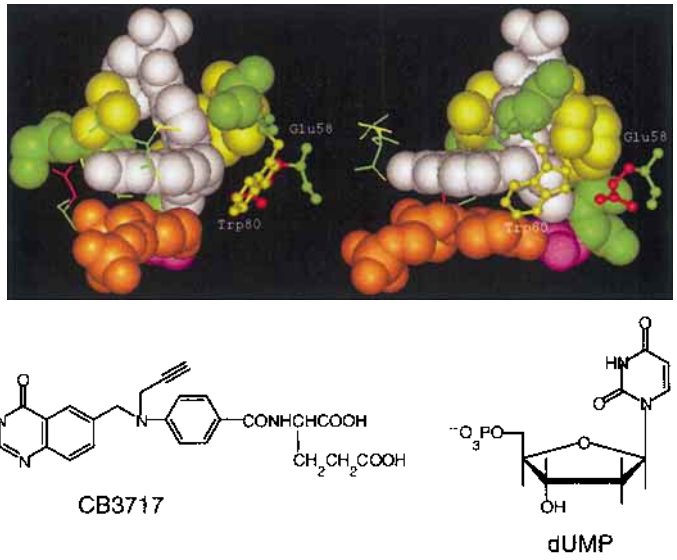

Fig. 3b. A Hydrophobic Space Surrounded by Glu58 and Trp80

The models viewed from two directions are shown. dUMP is shown by brown CPK model and CB3713 by white. The hydrophobic residues around CB3717 are also shown by CPK model. Glu58 and Trp80 are shown by ball-and-stick model.

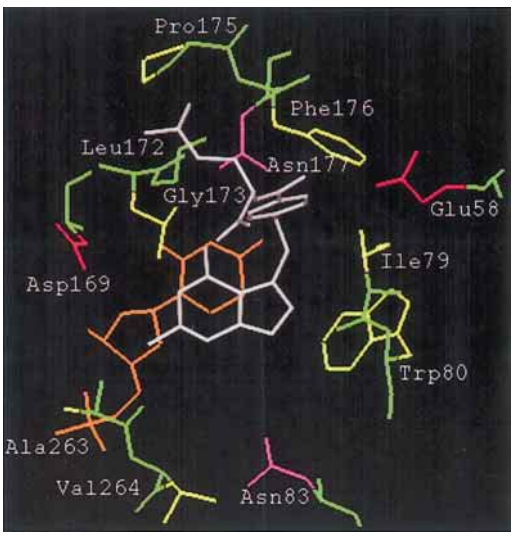

Fig. 4. A Schematic Model for Binding Mode of **2** with Human TS

Compound **2** is shown by white wire model and dUMP by brown.

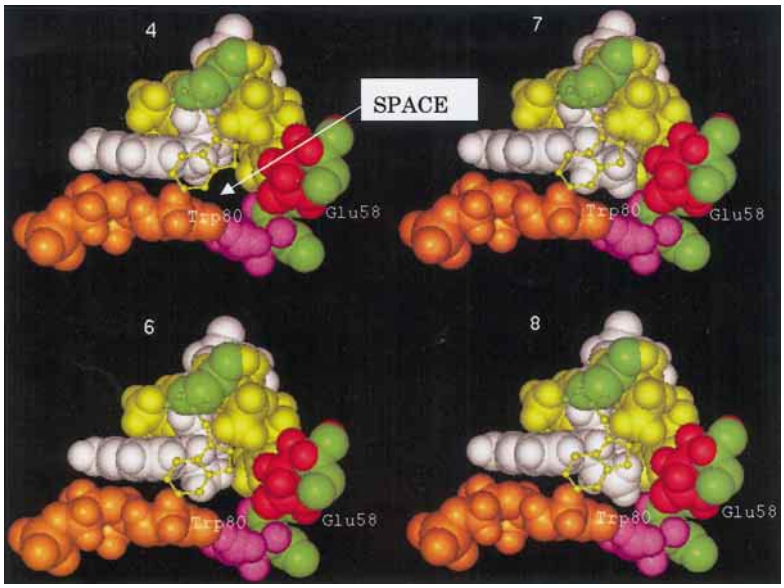

Fig. 7. Interaction of the C8 Substituents of **4**, **6**—**8** with the Hydrophobic Space Surrounded by Glu58 and Trp80

dUMP is shown by brown CPK model and inhibitors by white CPK model. The hydrophobic residues around the inhibitors and Glu58 are also shown by CPK model. Trp80 is shown by ball-and-stick model.

compounds **4** and **5** were prepared from the bromination of propionaldehydes **9a** and **9b**[8] by 5,5-dibromobarbituric acid (Chart 1). Condensation of 2,6-diamino-4-hydroxypyrimidine (**11**) and the α-bromoaldehydes **10a** and **10b** in DMSO containing K_2CO_3, gave pyrrolo[2,3-*d*]pyrimidines **12a** and **12b**. After acidic deprotection of the *tert*-butyl ester of **12a** and **12b** using trifluoroacetic acid (TFA), the resulting benzoic acids were coupled with diethyl L-glutamate using diethyl cyanophosphonate (DEPC). Basic hydrolysis of **13a** and **13b** with NaOH in H_2O–THF followed by an acid treatment gave the desired TS inhibitors **4** and **5**.

The synthetic pathway of compounds **6**—**8** is shown in Chart 2. These three compounds **6**—**8** were synthesized as racemates because they should bind to TS efficiently, regardless of the absolute configuration of C8. Wittig reaction of *tert*-butyl 4-formylbenzoate **14** with methyl (triphenylphosphoranyliden)acetate gave the cinnamate **15**. Treatment of the α,β-unsaturated ester **15** with lithium dimethylcuprate in the presence of trimethylchlorosilane[24] in anhydrous ether afforded the 1,4-addition product **16a**. The 1,4-adducts of ethyl **16b** or vinyl **16c** were synthesized by the conjugate addition using mixed cuprates [PhSCu(RMgBr)$_n$ (R=ethyl or vinyl)][25] prepared from cuprous thiophenoxide and the Grignard reagent. After selective reduction of methyl esters of

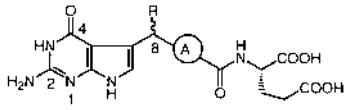

compound	A	R
4		H
5		H
6		CH_3
7		CH_2CH_3
8		$CH{=}CH_2$

Fig. 5. Pyrrolo[2,3-*d*]pyrimidine TS Inhibitors

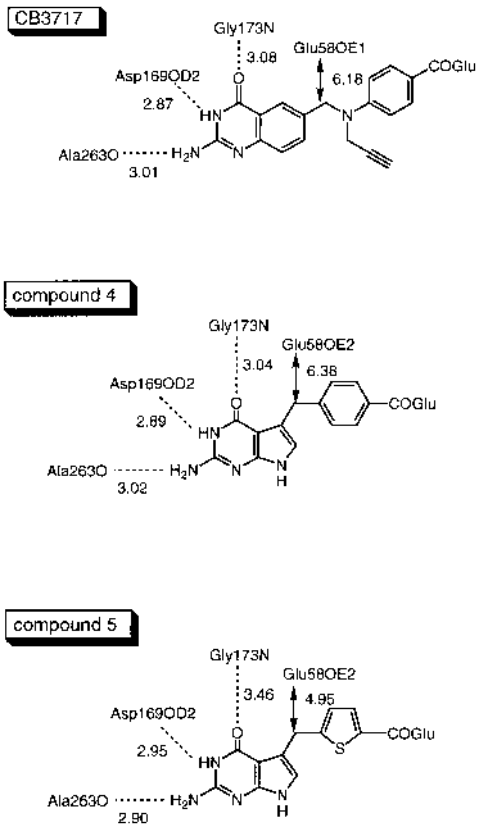

Fig. 6. Interaction Mode for TS-Inhibitor Complex

Hydrogen bonds are denoted by dashed lines with their distances (Å). The distances (Å) between Glu58 and the bridge carbon are indicated with arrows.

16a—**c** using lithium borohydride, the resulting alcohols **17a**—**c** were converted to the corresponding aldehydes **18a**—**c** by Swern's oxidation. The key intermediates **19a**—**c** were prepared by bromination using 5,5-dibromobarbituric acid. The remaining procedures used in the synthesis of the TS inhibitors **6**—**8** were similar to those for the syntheses of compounds **4** and **5** described above.

Biological Results and Discussion

Compounds **4** to **8** were evaluated for their inhibitory activities against TS purified from mouse fibrosarcoma Meth-A cells (Table 1). The amino acid sequence of the mouse enzyme has high homology (91% identity) to the human TS sequence and the active site region is exactly conserved (Fig. 2). Thus, it can be assumed that the activity of mouse TS is not significantly different from that of human TS.

Compound **4**, with the simple one-carbon bridge, showed moderate activity against TS, and its potency was almost 5-fold higher than that of compound **2** (LY231514) with the two-carbon bridge. Replacement of the benzene ring of **4** with its bioisoster thiophene (**5**) gave a 12-fold increase of TS inhibitory potency, which may be due to a favorable hydrophobic interaction of the bridge chain moiety caused by the replacement. The introduction of a hydrophobic substituent at C8 of **4** resulted in a 30—60 times improvement (**6**—**8**). The C8-ethyl analogue **7**, the most potent compound (IC_{50}=0.017 μM), possessed a 276-fold higher activity than **2** (LY231514). These results indicated that the substituent at C8 established a hydrophobic interaction and filled the unoccupied space created by Glu58, Trp80 and the bridge chain. The docking study to the human TS model was shown to be suitable for the design of potent TS inhibitors.

In conclusion, we designed the unique pyrrolo[2,3-*d*]pyrimidine TS inhibitors with one-carbon bridge based on the examination of the binding mode of compound **2** to the human TS model. During the course of these studies, five pyrrolo[2,3-*d*]pyrimidine derivatives (**4**—**8**) were synthesized and evaluated for their inhibitory activities against TS. They exhibited more potent TS inhibitory activities than compound **2** (LY231514). These results suggested that our modeling method was effective for designing novel and potent TS inhibitors.

Experimental

Melting points were determined on a Yanagimoto micro melting point apparatus and are uncorrected. ^{1}H-NMR spectra were recorded on a Varian Gemini-200 (200 MHz) instrument with tetramethylsilane as an internal standard. IR spectra were obtained on a JASCO IR-810 IR spectrophotometer. Secondary ionization mass spectra (SIMS) were measured on a Hitachi M-80A mass spectrometer. Elemental analyses were carried out by Takeda Analytical Research Laboratories, Ltd. Flash chromatography was performed on Merck silica gel 60 (230—400 mesh).

***tert*-Butyl 4-[(2-Amino-4-oxo-4,7-dihydro-3*H*-pyrrolo[2,3-*d*]pyrimidin-5-yl)methyl]benzoate (12a)** A mixture of *tert*-butyl 4-(3-oxopropyl)benzoate (11.52 g) and 5,5-dibromobarbituric acid (7.03 g) in Et_2O (225 ml) was stirred for 64 h at room temperature. The resulting precipitate was removed by filtration. The filtrate was washed with aqueous Na_2CO_3 and brine, dried over $MgSO_4$ and concentrated under vacuum to afford **10a** (12.51 g, 65%). To a solution of 2,4-diamino-6-hydroxypyrimidine (**11**, 1.45 g) in Me_2SO (6 ml) was added K_2CO_3 (60 mg), followed by addition of **10a** (3.00 g) in Me_2SO (5 ml). The mixture was stirred for 4 h at room temperature and then poured into water. The resulting precipitate was collected by filtration and purified by flash chromatography ($CHCl_3$/MeOH, 97 : 3) to give **12a** (1.43 g; 41%) as a white solid. IR (KBr): 3380, 3200, 3150, 2980, 1705, 1670, 1640, 1605, 1525 cm^{-1}. ^{1}H-NMR (Me_2SO-d_6) δ: 1.53 (9H, s), 3.99 (2H, s), 6.00 (2H, s), 6.32 (1H, s), 7.38 (2H, d, J=8.0 Hz), 7.77 (2H, d, J=8.0 Hz), 10.12 (1H, s), 10.72 (1H, s).

***tert*-Butyl 5-[(2-Amino-4-oxo-4,7-dihydro-3*H*-pyrrolo[2,3-*d*]pyrimidin-5-yl)methyl]thiophene-2-carboxylate (12b)** Compound **12b** (923 mg, 31%) as a white solid was synthesized from **9b** (2.42 g) by the same method as that described for **12a**. IR (KBr): 3420, 3320, 3200, 2980, 2920, 1680, 1600, 1605, 1540 cm^{-1}. ^{1}H-NMR (Me_2SO-d_6) δ: 1.48 (9H, s), 4.14 (2H, s), 6.05 (2H, s), 6.48 (1H, s), 6.95 (1H, d, J=3.8 Hz), 7.50 (2H, d, J=3.8 Hz), 10.19 (1H, s), 10.83 (1H, s).

Diethyl *N*-{4-[(2-Amino-4-oxo-4,7-dihydro-3*H*-pyrrolo[2,3-*d*]pyrimidin-5-yl)methyl]benzoyl}-L-glutamate (13a) Trifluoroacetic acid (0.6 ml) was added to a solution of **12a** (1.39 g) in CH_2Cl_2 (40 ml). The mixture was stirred for 4 h at room temperature and concentrated under vacuum. Triethylamine (1.62 g) was added dropwise to a solution of the resulting free acid, L-

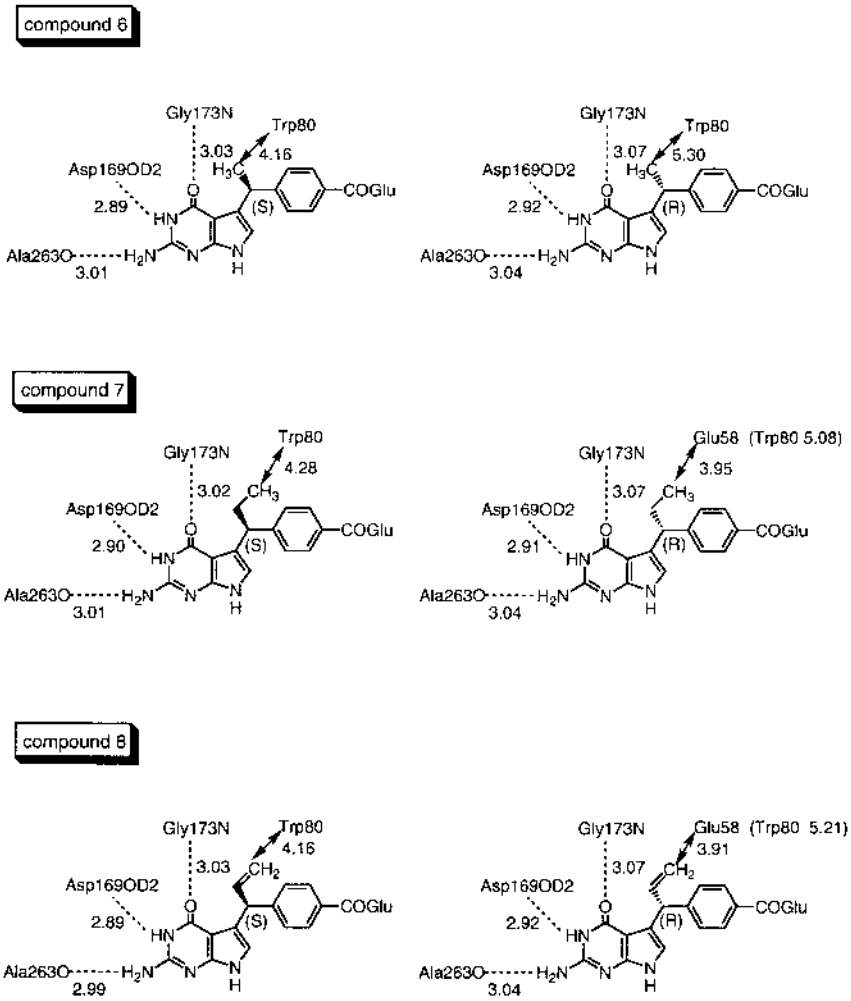

Fig. 8. Interaction Mode for TS–Inhibitor Complex

Hydrogen bonds are denoted by dashed lines with their distances (Å). The distances (Å) between Glu58 (Trp80) and C8 substituent are indicated with arrows.

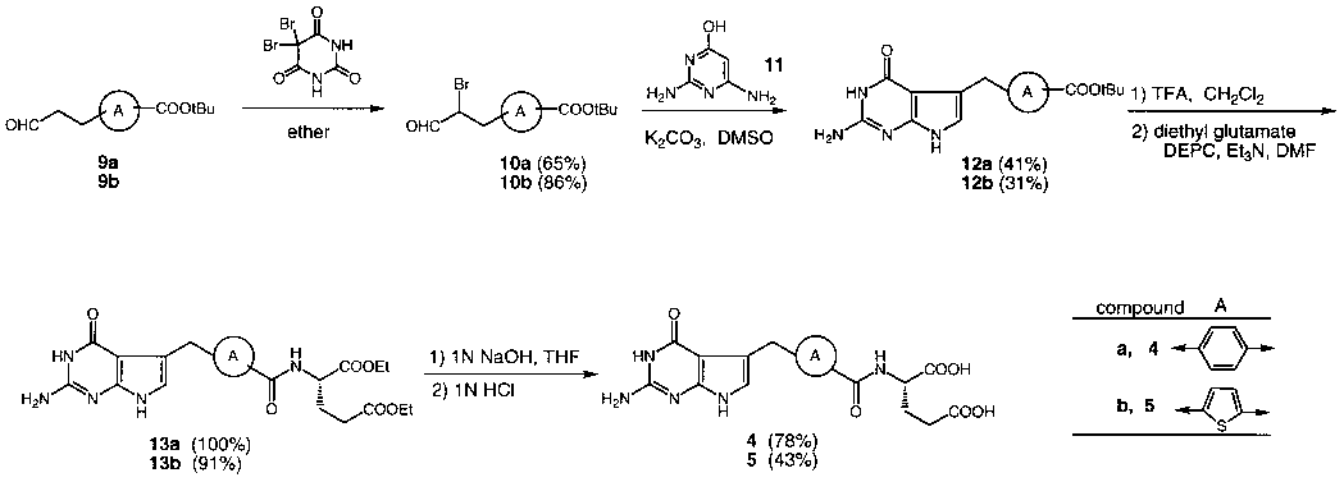

Chart 1. Synthesis of Pyrrolo[2,3-*d*]pyrimidine TS Inhibitors (**4**, **5**)

glutamic acid diethyl ester hydrochloride (1.20 g) and diethyl cyanophosphonate (DEPC, 0.72 g) in DMF (5 ml) with ice cooling. The mixture was stirred at room temperature for 18 h and diluted with AcOEt. The AcOEt solution was successively washed with 5% aqueous HCl solution, H_2O and brine, dried over $MgSO_4$ and concentrated under vacuum. The residue was purified by flash chromatography ($CHCl_3$/10% NH_3 in EtOH, 9 : 1) to give **13a** (1.70 g, 100%) as a white solid. IR (KBr): 3430, 3280, 3150, 2980, 1735, 1710, 1675, 1650, 1620, 1580, 1540 cm^{-1}. ^{1}H-NMR (Me_2SO-d_6) δ 1.16 (3H, t, J=7.0 Hz), 1.20 (3H, t, J=7.0 Hz), 1.95—2.15 (2H, m), 2.40 (2H, t, J=7.0 Hz), 3.99 (2H, s), 4.04 (2H, q, J=7.0 Hz), 4.10 (2H, q, J=7.0 Hz), 4.37—4.47 (1H, m), 5.99 (2H, s), 6.32 (1H, s), 7.37 (2H, d, J=8.0 Hz), 7.74 (2H, d, J=8.0 Hz), 8.85 (1H, d, J=7.0 Hz), 10.11 (1H, s), 10.71 (1H, s).

Diethyl *N*-({5-[(2-Amino-4-oxo-4,7-dihydro-3*H*-pyrrolo[2,3-*d*]pyrimidin-5-yl)methyl]thien-2-yl}carbonyl)-L-glutamate (13b) Compound **13b**

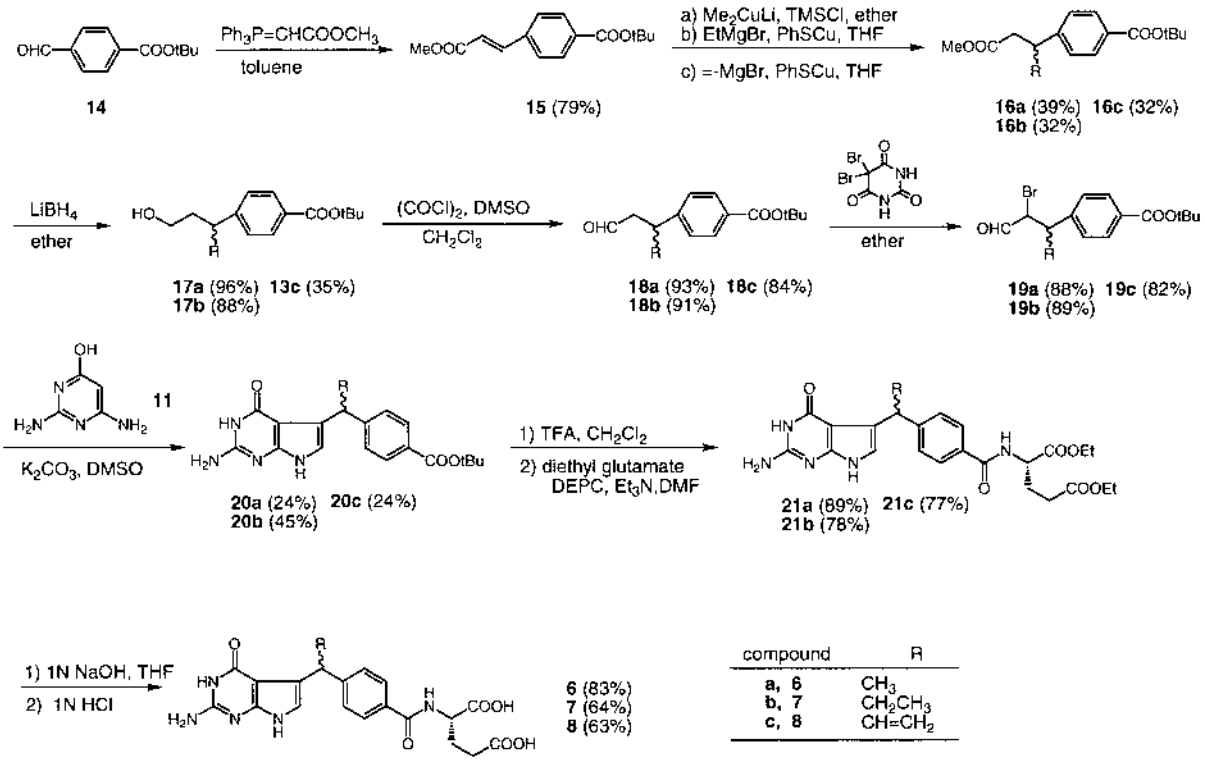

Chart 2. Synthesis of Pyrrolo[2,3-*d*]pyrimidine TS Inhibitors (**6**—**8**)

Table 1. Inhibition of Thymidylate Synthase

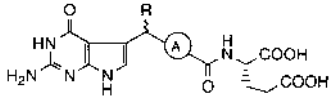

Compound	R	A	IC_{50} (μM) TS
4	H		1.0
5	H		0.083
6	CH_3		0.039
7	CH_2CH_3		0.017
8	$CH{=}CH_2$		0.037
2 (LY231514)	H	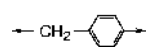	4.7

(1.01 g, 91%) as a white solid was synthesized from **12b** (2.42 g) by the same method as that described for **13a**. IR (KBr): 3300, 3210, 2980, 2940, 1735, 1710—1580 cm^{-1}. ^{1}H-NMR (Me_2SO-d_6) δ: 1.16 (3H, t, J=7.0 Hz), 1.18 (3H, t, J=7.0 Hz), 1.91—2.20 (2H, m), 2.42 (2H, t, J=7.0 Hz), 4.13 (2H, s), 4.04 (2H, q, J=7.0 Hz), 4.10 (2H, q, J=7.0 Hz), 4.32—4.45 (1H, m), 6.10 (2H, s), 6.45 (1H, s), 6.91 (1H, d, J=4.0 Hz), 7.65 (1H, d, J=4.0 Hz), 8.58 (1H, d, J=7.0 Hz), 10.22 (1H, s), 10.82 (1H, s).

***N*-{4-[(2-Amino-4-oxo-4,7-dihydro-3*H*-pyrrolo[2,3-*d*]pyrimidin-5-yl)-methyl]benzoyl}-L-glutamic Acid (4)** A solution of **13a** (1.70 g) in H_2O–THF (1 : 1, 36 ml) was treated with 1 N aqueous NaOH solution (14.5 ml) at room temperature for 4 h. THF was evaporated under vacuum and 1 N HCl solution was added dropwise to the residue. The white crystalline precipitate was collected by filtration, washed successively with water, MeOH and ether and dried over P_2O_5 under vacuum to give **4** (1.40 g, 78%). mp 186—189 °C. IR (KBr): 3320, 2930, 1700, 1650, 1650, 1535, 1500 cm^{-1}. ^{1}H-NMR (Me_2SO-d_6) δ: 1.85—2.20 (2H, m), 2.34 (2H, t, J=7.0 Hz), 3.98 (2H, s), 4.34—4.47 (1H, m), 5.99 (2H, s), 6.32 (1H, s), 7.37 (2H, d, J=8.0 Hz), 7.75 (2H, d, J=8.0 Hz), 8.46 (1H, d, J=8.0 Hz), 10.13 (1H, s), 10.71 (1H, s). Secondary ion mass spectrometry (SIMS) *m/z* 414 (MH^+). *Anal*. Calcd for $C_{19}H_{19}N_5O_6 \cdot 0.7H_2O$: C, 53.57; H, 4.83; N, 16.44. Found: C, 53.53; H, 4.96; N, 16.31.

***N*-({5-[(2-Amino-4-oxo-4,7-dihydro-3*H*-pyrrolo[2,3-*d*]pyrimidin-5-yl)-methyl]thien-2-yl}carbonyl)-L-glutamic Acid (5)** Compound **5** (416 mg, 43%) as a white crystalline solid was synthesized from **13b** (1.10 g) by the same method as that described for **13a**. mp 179—182 °C. IR (KBr): 3350, 3240, 2930, 1700—1640, 1540 cm^{-1}. ^{1}H-NMR (Me_2SO-d_6) δ: 1.81—2.19 (2H, m), 2.22—2.47 (2H, m), 4.14 (2H, s), 4.24—4.41 (1H, m), 6.05 (2H, s), 6.45 (1H, s), 6.91 (1H, d, J=2.8 Hz), 7.65 (1H, d, J=2.8 Hz), 8.45 (1H, d, J=7.0 Hz), 10.18 (1H, s), 10.81 (1H, s). SIMS *m/z* 420 (MH^+). *Anal*. Calcd for $C_{17}H_{17}N_5O_6S \cdot 0.5H_2O$: C, 47.66; H, 4.23; N, 16.35. Found: C, 47.60; H, 4.35; N, 16.21.

***tert*-Butyl 4-[(1*E*)-3-Methoxy-3-oxo-1-propenyl]benzoate (15)** A mixture of *tert*-butyl 4-formylbenzoate (**14**, 75 g) and methyl (triphenylphoranyliden)acetate (122 g) in toluene (1 l) was refluxed for 2 h. The insoluble material was removed by filtration. The filtrate was concentrated under vacuum. The residue was triturated with MeOH. The resulting white precipitate was collected by filtration, washed with MeOH and ether and dried under vacuum to give **15** (74.5 g, 78%). IR (KBr): 2950, 1710, 1640, 1600, 1560 cm^{-1}. ^{1}H-NMR ($CDCl_3$) δ: 1.69 (9H, s), 3.82 (3H, s), 6.50 (1H, d, J=16.0 Hz), 7.55 (2H, d, J=8.4 Hz), 7.70 (1H, d, J=16.0 Hz), 7.99 (2H, d, J=8.4 Hz).

***tert*-Butyl 4-(3-Methoxy-1-methyl-3-oxopropyl)benzoate (16a)** Under an argon atmosphere methyllithium (1.5 M solution in Et_2O, 64 ml) was added dropwise to a suspension of copper(I) iodide (9.14 g) in anhydrous Et_2O at −40 °C. To the solution of Me_2CuLi were added successively trimethylchlorosilane (6.7 ml) and **15** (10.49 g) in anhydrous Et_2O (300 ml) at −78 °C. The stirred mixture was allowed to warm slowly up to room temperature (1 h). Stirring was continued at room temperature for 2 h, then hydrolyzed with aqueous NH_4Cl. The aqueous layer was extracted with Et_2O. The combined ether layer was washed with brine, dried over $MgSO_4$ and concentrated under vacuum. The residue was purified by flash chromatography (*n*-hexane/AcOEt, 95 : 5) to afford **16a** (4.36 g, 39%) as a colorless oil. IR (KBr): 2980, 2940, 1710, 1720, 1605 cm^{-1}. ^{1}H-NMR ($CDCl_3$) δ: 1.30

(3H, d, J=7.0 Hz), 1.58 (9H, s), 2.55 (1H, dd, J=7.6, 15.5 Hz), 2.64 (1H, dd, J=7.6, 15.5 Hz), 3.23—3.43 (1H, m), 3.61 (3H, s), 7.26 (2H, d, J=8.6 Hz), 7.92 (2H, d, J=8.6 Hz).

***tert*-Butyl 4-(1-Ethyl-3-Methoxy-3-oxopropyl)benzoate (16b)** Under an argon atmosphere ethylmagnesium bromide (1.0 M solution in THF, 85 ml) was added dropwise to a suspension of phenylthiocopper (5.79 g) in anhydrous THF at −40 °C. The mixture was allowed to warm up to −15 °C. After a solution of **15** (7.50 g) in anhydrous THF (50 ml) was added dropwise, the mixture was stirred at 0 °C for 1 h and poured into aqueous NH_4Cl. The precipitate was removed by filtration. The filtrate was extracted with Et_2O. The combined ether layer was washed with brine, dried over $MgSO_4$ and concentrated under vacuum. The residue was purified by flash chromatography (*n*-hexane/AcOEt, 95 : 5) to afford **16b** (2.68 g, 32%) as a colorless oil. IR (KBr): 2960, 2930, 1740, 1705, 1605 cm^{-1}. ^{1}H-NMR ($CDCl_3$) δ: 0.78 (3H, t, J=7.4 Hz), 1.59 (9H, s), 1.53—1.78 (2H, m), 2.57 (1H, dd, J=8.4, 15.0 Hz), 2.68 (1H, dd, J=6.5, 15.0 Hz), 2.93—3.17 (1H, m), 3.57 (3H, s), 7.23 (2H, d, J=8.2 Hz), 7.92 (2H, d, J=8.2 Hz).

***tert*-Butyl 4-[1-(2-Methoxy-2-oxoethyl)-2-propenyl]benzoate (16c)** Compound **16c** (2.39 g, 31%) as a colorless oil was synthesized from **15** (7.00 g) by the same method as that described for **16b**. IR (KBr): 2980, 1740, 1640, 1605 cm^{-1}. ^{1}H-NMR ($CDCl_3$) δ: 1.58 (9H, s), 1.53—1.78 (2H, m), 2.70 (1H, dd, J=7.8, 15.4 Hz), 2.80 (1H, dd, J=7.8, 15.4 Hz), 3.61 (3H, s), 3.86—3.89 (1H, m), 5.06 (1H, dt, J=16.8, 1.2 Hz), 5.10 (1H, dt, J=10.6, 1.2 Hz), 5.96 (1H, ddd, J=16.8, 10.6, 6.8 Hz), 7.26 (2H, d, J=8.4 Hz), 7.93 (2H, d, J=8.4 Hz).

***tert*-Butyl 4-(3-Hydroxy-1-methylpropyl)benzoate (17a)** Lithium borohydride (348 mg) was added to a solution of **16a** (4.24 g) in anhydrous Et_2O (30 ml). After the mixture was stirred at room temperature for 13 h, the reaction was quenched with 1 N aqueous $KHSO_4$ solution. The aqueous layer was extracted with Et_2O. The combined ether layer was washed with brine, dried over $MgSO_4$ and concentrated under vacuum. The residue was purified by flash chromatography (*n*-hexane/AcOEt, 4 : 1) to afford **17a** (3.56 g, 96%) as a colorless oil. IR (KBr): 3400, 2980, 2940, 2880, 1720, 1610 cm^{-1}. ^{1}H-NMR ($CDCl_3$) δ: 1.28 (3H, d, J=7.0 Hz), 1.39 (1H, m), 1.59 (9H, s), 1.80—1.91 (2H, m), 2.86—3.06 (1H, m), 3.50 (1H, dd, J=6.6, 10.6 Hz), 3.61 (1H, dd, J=6.6, 10.6 Hz), 7.25 (2H, d, J=8.2 Hz), 7.93 (2H, d, J=8.2 Hz).

***tert*-Butyl 4-(3-Hydroxy-1-ethylpropyl)benzoate (17b)** Compound **17b** (1.07 g, 88%) as a colorless oil was synthesized from **16b** (1.34 g) by the same method as that described for **17a**. IR (KBr): 3400, 2970, 2930, 2860, 1710, 1605 cm^{-1}. ^{1}H-NMR ($CDCl_3$) δ: 0.77 (3H, t, J=7.4 Hz), 1.34—1.51 (1H, m), 1.59 (9H, s), 1.61—1.99 (4H, m), 2.60—2.76 (1H, m), 3.37—3.60 (2H, m), 7.21 (2H, d, J=8.2 Hz), 7.92 (2H, d, J=8.2 Hz).

***tert*-Butyl 4-[1-(2-Hydroxyethyl)-2-propenyl]benzoate (17c)** Compound **17c** (791 mg, 35%) as a colorless oil was synthesized from **16c** (2.38 g) by the same method as that described for **17a**. IR (KBr): 3400, 2980, 2940, 1715, 1640, 1605 cm^{-1}. ^{1}H-NMR ($CDCl_3$) δ: 1.28—1.38 (1H, m), 1.59 (9H, s), 1.87—2.09 (2H, m), 3.47—3.68 (3H, m), 5.08 (1H, dt, J=10.0, 1.4 Hz), 5.08 (1H, dt, J=17.0, 1.4 Hz), 5.96 (1H, ddd, J=17.0, 10.0, 7.8 Hz), 7.25 (2H, d, J=8.2 Hz), 7.93 (2H, d, J=8.2 Hz).

***tert*-Butyl 4-(1-Methyl-3-oxopropyl)benzoate (18a)** Under an argon atmosphere a solution of DMSO (2.57 g) in CH_2Cl_2 (35 ml) was added to a solution of oxalyl chloride (2.09 g) in CH_2Cl_2 (70 ml) at −60 °C. After 2 min, a solution of **17a** (3.43 g) in CH_2Cl_2 (30 ml) was added. Stirring was continued at −60 °C for 15 min, and then triethylamine (6.93 g) was added. The mixture was allowed to warm to 0 °C in 30 min, and poured into water (350 ml). The aqueous phase was extracted with CH_2Cl_2. The combined organic phase was dried over $MgSO_4$ and concentrated under vacuum. Purification by flash chromatography (*n*-hexane/AcOEt, 5 : 1) gave **18a** (3.16 g, 93%) as a colorless oil. IR (KBr): 2980, 2840, 1735, 1715, 1610 cm^{-1}. ^{1}H-NMR ($CDCl_3$) δ: 1.32 (3H, d, J=6.8 Hz), 1.59 (9H, s), 2.68 (1H, ddd, J=16.8, 6.8, 1.8 Hz), 2.78 (1H, ddd, J=16.8, 6.8, 1.8 Hz), 3.32—3.52 (1H, m), 7.27 (2H, d, J=8.4 Hz), 7.94 (2H, d, J=8.4 Hz), 9.72 (1H, t, J=1.8 Hz).

***tert*-Butyl 4-(1-Ethyl-3-oxopropyl)benzoate (18b)** Compound **18b** (955 mg, 91%) as a colorless oil was synthesized from **17b** (1.06 g) by the same method as that described for **18a**. IR (KBr): 2970, 2930, 1700, 1605 cm^{-1}. ^{1}H-NMR ($CDCl_3$) δ: 0.80 (3H, t, J=7.2 Hz), 1.59 (9H, s), 1.61—1.78 (2H, m), 2.74 (1H, dd, J=7.4, 1.8 Hz), 3.07—3.23 (1H, m), 7.24 (2H, d, J=8.4 Hz), 7.93 (2H, d, J=8.2 Hz), 9.67 (1H, t, J=1.8 Hz).

***tert*-Butyl 4-[1-(2-Oxoethyl)-2-propenyl]benzoate (18c)** Compound **18c** (635 mg, 84%) as a colorless oil was synthesized from **17c** (784 mg) by the same method as that described for **18a**. IR (KBr): 2980, 1725, 1715, 1640, 1605 cm^{-1}. ^{1}H-NMR ($CDCl_3$) δ: 1.58 (9H, s), 2.81 (1H, ddd, J=17.0, 7.5, 1.8 Hz), 2.91 (1H, ddd, J=17.0, 7.5, 1.8 Hz), 3.95—4.07 (1H, m), 5.08 (1H, dt, J=17.0, 1.0 Hz), 5.14 (1H, dt, J=10.6, 1.0 Hz), 5.97 (1H, ddd, J=17.0, 10.6, 6.8 Hz), 7.26 (2H, d, J=8.0 Hz), 7.94 (2H, d, J=8.0 Hz), 9.72 (1H, t, J=1.8 Hz).

***tert*-Butyl 4-[1-(2-Amino-4-oxo-4,7-dihydro-3*H*-pyrrolo[2,3-*d*]pyrimidin-5-yl)ethyl]benzoate (20a)** Compound **20a** (916 mg, 24%) as a white solid was synthesized from **18a** (3.03 g) by the same method as that described for **12a**. IR (KBr): 3340, 3200, 3150, 2980, 2940, 1720, 1640, 1600, 1540 cm^{-1}. ^{1}H-NMR (Me_2SO-d_6) δ: 1.52 (9H, s), 1.54 (3H, d, J=8.0 Hz), 4.34—4.48 (1H, m), 5.92 (2H, s), 6.34 (1H, d, J=1.6 Hz), 7.40 (2H, d, J=8.2 Hz), 7.77 (2H, d, J=8.2 Hz), 10.05 (1H, s), 10.73 (1H, d, J=1.6 Hz).

***tert*-Butyl 4-[1-(2-Amino-4-oxo-4,7-dihydro-3*H*-pyrrolo[2,3-*d*]pyrimidin-5-yl)propyl]benzoate (20b)** Compound **20b** (510 mg, 45%) as a white solid was synthesized from **18b** (911 mg) by the same method as that described for **12a**. IR (KBr): 3330, 3200, 1710, 1665, 1600, 1520 cm^{-1}. ^{1}H-NMR (Me_2SO-d_6) δ: 0.80 (3H, t, J=7.2 Hz), 1.52 (9H, s), 1.83—1.98 (1H, m), 2.08—2.23 (1H, m), 4.15 (1H, t, J=8.2 Hz), 5.98 (2H, s), 6.40 (1H, d, J=1.8 Hz), 7.43 (2H, d, J=8.2 Hz), 7.77 (2H, d, J=8.2 Hz), 10.06 (1H, s), 10.74 (1H, d, J=1.8 Hz).

***tert*-Butyl 4-[1-(2-Amino-4-oxo-4,7-dihydro-3*H*-pyrrolo[2,3-*d*]pyrimidin-5-yl)-2-propenyl]benzoate (20c)** Compound **20c** (171 mg, 24%) as a white solid was synthesized from **18c** (622 mg) by the same method as that described for **12a**. IR (KBr): 3340, 3200, 2980, 1705, 1670, 1635, 1600, 1540 cm^{-1}. ^{1}H-NMR (Me_2SO-d_6) δ: 1.52 (9H, s), 4.99—5.05 (1H, m), 5.00 (1H, d, J=17.0 Hz), 5.06 (1H, d, J=10.0 Hz), 6.01 (2H, s), 6.43 (1H, ddd, J=17.0, 10.0, 8.0 Hz), 6.45 (1H, s), 7.33 (2H, d, J=8.2 Hz), 7.78 (2H, d, J=8.2 Hz), 10.07 (1H, s), 10.83 (1H, d, J=2.2 Hz).

Diethyl *N*-{4-[1-(2-Amino-4-oxo-4,7-dihydro-3*H*-pyrrolo[2,3-*d*]pyrimidin-5-yl)ethyl]benzoyl}-L-glutamate (21a) Compound **21a** (974 mg, 89%) as a white solid was synthesized from **20a** (800 mg) by the same method as that described for **13a**. IR (KBr): 3350, 2970, 2920, 1735, 1680—1580, 1500 cm^{-1}. ^{1}H-NMR (Me_2SO-d_6) δ: 1.16 (3H, t, J=7.2 Hz), 1.18 (3H, t, J=7.2 Hz), 1.55 (3H, d, J=7.4 Hz), 1.94—2.18 (2H, m), 2.42 (2H, t, J=7.4 Hz), 4.05 (2H, q, J=7.2 Hz), 4.10 (2H, q, J=7.2 Hz), 4.30—4.49 (2H, m), 5.98 (2H, s), 6.34 (1H, d, J=1.6 Hz), 7.39 (2H, d, J=8.4 Hz), 7.75 (2H, d, J=8.4 Hz), 8.58 (1H, d, J=7.6 Hz), 10.05 (1H, s), 10.71 (1H, t, J=1.6 Hz).

Diethyl *N*-{4-[1-(2-Amino-4-oxo-4,7-dihydro-3*H*-pyrrolo[2,3-*d*]pyrimidin-5-yl)propyl]benzoyl}-L-glutamate (21b) Compound **21b** (528 mg, 78%) as a white solid was synthesized from **20b** (500 mg) by the same method as that described for **13a**. IR (KBr): 3300, 3240, 3150, 2960, 2925, 1730, 1680, 1650, 1625, 1600 cm^{-1}. ^{1}H-NMR (Me_2SO-d_6) δ: 0.81 (3H, t, J=7.0 Hz), 1.16 (3H, t, J=7.0 Hz), 1.18 (3H, t, J=7.0 Hz), 1.84—2.23 (4H, m), 2.42 (2H, t, J=7.4 Hz), 4.04 (2H, q, J=7.0 Hz), 4.10 (2H, q, J=7.0 Hz), 4.11—4.19 (1H, m), 4.30—4.49 (1H, m), 5.98 (2H, s), 6.40 (1H, d, J=1.4 Hz), 7.41 (2H, d, J=8.4 Hz), 7.74 (2H, d, J=8.4 Hz), 8.58 (1H, d, J=7.8 Hz), 10.06 (1H, s), 10.72 (1H, t, J=1.4 Hz).

Diethyl *N*-{4-[1-(2-Amino-4-oxo-4,7-dihydro-3*H*-pyrrolo[2,3-*d*]pyrimidin-5-yl)-2-propenyl]benzoyl}-L-glutamate (21c) Compound **21c** (171 mg, 77%) as a white solid was synthesized from **20c** (165 mg) by the same method as that described for **13a**. IR (KBr): 3350, 3215, 2980, 1740, 1680—1600, 1540, 1500 cm^{-1}. ^{1}H-NMR (Me_2SO-d_6) δ: 1.16 (3H, t, J=7.0 Hz), 1.18 (3H, t, J=7.0 Hz), 1.92—2.16 (2H, m), 2.42 (2H, t, J=7.4 Hz), 4.04 (2H, q, J=7.0 Hz), 4.09 (2H, q, J=7.0 Hz), 4.33—4.44 (1H, m), 4.99 (1H, d, J=16.4 Hz), 5.04 (1H, d, J=10.0 Hz), 5.01—5.07 (1H, m), 6.00 (2H, s), 6.43 (1H, d, J=1.6 Hz), 6.44 (1H, ddd, J=16.4, 10.0, 8.2 Hz), 7.31 (2H, d, J=8.4 Hz), 7.74 (2H, d, J=8.4 Hz), 8.58 (1H, d, J=7.6 Hz), 10.07 (1H, s), 10.81 (1H, t, J=1.6 Hz).

***N*-{4-[1-(2-Amino-4-oxo-4,7-dihydro-3*H*-pyrrolo[2,3-*d*]pyrimidin-5-yl)ethyl]benzoyl}-L-glutamic Acid (6)** Compound **6** (674 mg, 83%) as a white crystalline solid was synthesized from **21a** (920 mg) by the same method as that described for **4**. mp 187—191 °C. IR (KBr): 3350, 3200, 2960, 1700, 1660 cm^{-1}. ^{1}H-NMR (Me_2SO-d_6) δ: 1.55 (3H, d, J=7.2 Hz), 1.88—2.18 (2H, m), 2.34 (2H, t, J=7.4 Hz), 4.31—4.47 (2H, m), 5.98 (2H, s), 6.32 (1H, s), 7.38 (2H, d, J=8.2 Hz), 7.75 (2H, d, J=8.2 Hz), 8.45 (1H, d, J=8.0 Hz), 10.04 (1H, s), 10.70 (1H, s). SIMS *m/z* 428 (MH^+). *Anal*. Calcd for $C_{20}H_{21}N_5O_6 \cdot 0.5H_2O$: C, 55.04; H, 5.08; N, 16.05. Found: C, 54.92; H, 5.29; N, 16.04.

***N*-{4-[1-(2-Amino-4-oxo-4,7-dihydro-3*H*-pyrrolo[2,3-*d*]pyrimidin-5-yl)propyl]benzoyl}-L-glutamic Acid (7)** Compound **7** (292 mg, 64%) as a white solid was synthesized from **21b** (500 mg) by the same method as that described for **4**. mp 116—119 °C. IR (KBr): 3350, 2960, 2920, 1700—1600, 1530 cm^{-1}. ^{1}H-NMR (Me_2SO-d_6) δ: 0.80 (3H, t, J=7.4 Hz), 1.81—2.21 (4H, m), 2.34 (2H, t, J=7.4 Hz), 4.14 (2H, q, J=7.4 Hz), 4.31—4.45 (1H, m), 5.97 (2H, s), 6.39 (1H, d, J=1.4 Hz), 7.40 (2H, d, J=8.2 Hz), 7.74 (2H, d, J=8.2 Hz), 8.45 (1H, d, J=8.2 Hz), 10.05 (1H, s), 10.71 (1H, s). SIMS

m/z 442 (MH^+). *Anal*. Calcd for $C_{21}H_{23}N_5O_6 \cdot 0.5H_2O$: C, 56.00; H, 5.37; N, 15.55. Found: C, 56.02; H, 5.55; N, 15.62.

***N*-{4-[1-(2-Amino-4-oxo-4,7-dihydro-3*H*-pyrrolo[2,3-*d*]pyrimidin-5-yl)-2-propenyl]benzoyl}-L-glutamic Acid (8)** Compound **8** (82 mg, 77%) as a white solid was synthesized from **21c** (146 mg) by the same method as that described for **4**. mp 180—183 °C. IR (KBr): 3350, 2940, 1700—1600, 1540 cm^{-1}. ^{1}H-NMR (Me_2SO-d_6) δ: 1.87—2.18 (2H, m), 2.34 (2H, t, J=7.2 Hz), 4.34—4.45 (1H, m), 4.95—5.12 (3H, m), 6.00 (2H, s), 6.34—6.53 (1H, m), 6.44 (1H, s), 7.31 (2H, d, J=8.0 Hz), 7.75 (2H, d, J=8.0 Hz), 8.46 (1H, d, J=7.8 Hz), 10.07 (1H, s), 10.81 (1H, s). SIMS *m/z* 440 (MH^+). *Anal*. Calcd for $C_{21}H_{21}N_5O_6 \cdot 0.7H_2O$: C, 55.79; H, 4.99; N, 15.49. Found: C, 55.98; H, 5.25; N, 15.50.

Preparation of Crude TS A crude fraction of TS was prepared from Meth-A fibrosarcoma cells. Meth-A cells (2×10^4 ml), in 2.0 l of Eagle's minimum essential medium (MEM) supplemented with 10% fetal bovine serum (FBS), were divided into ten culture flasks and incubated for 72 h at 37 °C in 5% CO_2. Cells were washed twice in phosphate-buffered saline and resuspended in 5 ml of 250 mM sucrose, 10 mM Tris–HCl buffer (ph 7.5), and then disrupted ultrasonically. Cell lysate was centrifuged at 100000×***g*** for 1 h at 4 °C. The cytosol fraction (crude TS fraction) was diluted with 250 mM sucrose and 10 mM Tris–HCl buffer (pH 7.5) to adjust the protein concentration to 10 mg/ml and then it was stored at −20 °C.

TS Inhibition Assay TS activity was measured by the method of Roberts[26] with some modification. In brief, 10 μl of crude TS fraction was added to 40 μl of reaction mixture in a flat-bottom 96 well plate, in triplicate. The final concentrations of the constituents of the reaction mixture were as follows; 800 μM tetrahydrofolic acid, 18 mM formaldehyde, 80 μM dUMP, 0.51 μM [^{3}H]dUMP, 10.2 mM 2-mercaptoethanol, 100 mM sucrose, 68 mM NaF, 174 mM Tris–HCl (pH 7.5), 6.24 mg/ml bovine serum albumin and various concentrations of test compounds. The reaction mixture was incubated on a water bath at 37 °C for 1 h and then chilled on ice. Ice cold 26.65% trichloroacetic acid (20 μl), 3.33 mg/ml cold dUMP (10 μl) and 114 mg/ml charcoal (220 μl) were added to the reaction mixture, which was then transferred to a centrifuge tube. After centrifugation, the amount of [^{3}H]H_2O released from [^{3}H]dUMP in the supernatant of the reaction mixture was measured using a liquid scintillation counter.

Acknowledgements We are grateful to Drs. T. Aono and T. Miwa for their encouragement and valuable advice. We thank Mr. T. Hitaka for his excellent technical support.

References and Notes

1) Christopherson R. O., Lyons S. D., *Medicinal Research Reviews*, **10**, 505—548 (1990).
2) Brandt D. S., Chu E., *Oncology Research*, **9**, 403—410 (1997).
3) Miwa T., Hitaka T., Akimoto H., Nomura H., *J. Med. Chem*., **34**, 555—560 (1991).
4) Akimoto H., Hitaka T., Miwa T., Yukishige K., Kusanagi T., Ootsu K., *Pro. Am. Cancer Res*., **32**, 327 (1991).
5) Yukishige K., Kusanagi T., Fujita T., Aso K., Akimoto H., Ootsu K., *Proc. Jpn. Cancer Assoc*., **1991**, 385.
6) Itoh F., Russello O., Akimoto H., Beardsley G. P., *Cancer Chemother. Pharmacol*., **43**, 230—235 (1994).
7) Yukishige K., Wajima M., Kusanagi T., Aso K., Akimoto H., Ootsu, K., *J. Takeda Res. Lab*., **54**, 97—107 (1995).
8) Miwa T., Hitaka T., Akimoto H., *J. Org. Chem*., **58**, 1696—1701 (1993).
9) Aso K., Hitaka T., Yukishige K., Ootsu K., Akimoto H., *Chem. Pharm. Bull*., **43**, 256—261 (1995).
10) Itoh F., Yukishige K., Wajima M., Ootsu K., Akimoto H., *Chem. Pharm. Bull*., **43**, 230—235 (1995).
11) Itoh F., Yoshioka K., Yukishige K., Yoshida M., Wajima M., Ootsu K., Akimoto H., *Chem. Pharm. Bull*., **44**, 1498—1509 (1996).
12) Itoh F., Yoshioka K., Yukishige K., Yoshida M., Ootsu K., Akimoto H., *Chem. Pharm. Bull*., **48**, 1271—1281 (2000).
13) Taylor E. C., Harrington P. J., Fletcher S. R., Beardsley G. P., Moran, R. G., *J. Med. Chem*., **28**, 914—921 (1985).
14) Taylor E. C., Kuhnt D., Shih C., Rinzel S. M., Grindey G. B., Barredo J., Jannatipour M., Moran R. G., *J. Med. Chem*., **35**, 4450—4454 (1992).
15) John W., Picus J., Blanke C. D., Clark J. W., Schulman L. N., Rowinsky E. K., Thornton D. E., Loehrer P. J., *Cancer*, **88**, 1807—1813 (2000).
16) Montfort W. R., Perry K. M., Fauman E. B., Finer-Moore J. S., Maley G. F., Hardy L., Maley F., Stroud R. M., *Biochemistry*, **29**, 6964—6977 (1990).
17) Appelt K., Bacquet R. J., Bartlett C. A., Booth C. L. J., Freer S. T., Fuhry M. A. M., Gehring M. R., Herrmann S. M., Howland E. F., Janson C. A., Jones T. R., Kan C.-C., Kathardekar V., Lewis K. K., Marzoni G. P., Matthews D. A., Mohr C., Moomaw E. W., Morse C. A., Oatley S. J., Ogden R. C., Reddy M. R., Reich S. H., Schoettlin W. S., Smith W. W., Varney M. D., Villafanca J. E., Ward R. W., Webber S., Webber S. E., Welsh K. M., White J., *J. Med. Chem*., **34**, 1925—1934 (1991).
18) Protein Data Bank ID code: 2TSC.
19) The modeling studies were performed on a Silicon Graphics IRIS 4D/220GTX workstation (Silicon Graphics Inc., Mountain View, CA, U.S.A.) with the Insight II/Discover program package (Accelrys Inc., Princeton, NJ, U.S.A.).
20) Protein Data Bank ID codes: 1HVY, 1HW3 and 1HW4.
21) The average pairwise root mean square deviation (RMSD) for the backbone was 2.06 Å. The RMSD for the backbone at the active site was 0.65 Å.
22) Gangjee A., Devraj R., McGuire J. J., Kisliuk R. L., *J. Med. Chem*., **38**, 4495—4502 (1995).
23) Secrist III, J. A., Liu P. S., *J. Org. Chem*., **43**, 3937—3941 (1978).
24) Alexakis A., Berlan J., Besace Y., *Tetrahedron Lett*., **27**, 1047—1050 (1986).
25) Behforouz M., Curran T. T., Bolan J. L., *Tetrahedron Lett*., **27**, 3107—3110 (1986).
26) Roberts D., *Biochemistry*, **5**, 3546—3548 (1966).